

1-1-1957

# Operating characteristics of a uranium graphite subcritical assembly ...

Fred Hubbard Baughman  
*Iowa State College*

Follow this and additional works at: <https://lib.dr.iastate.edu/rtd>



Part of the [Engineering Commons](#)

---

## Recommended Citation

Baughman, Fred Hubbard, "Operating characteristics of a uranium graphite subcritical assembly ..." (1957). *Retrospective Theses and Dissertations*. 18027.  
<https://lib.dr.iastate.edu/rtd/18027>

This Thesis is brought to you for free and open access by the Iowa State University Capstones, Theses and Dissertations at Iowa State University Digital Repository. It has been accepted for inclusion in Retrospective Theses and Dissertations by an authorized administrator of Iowa State University Digital Repository. For more information, please contact [digirep@iastate.edu](mailto:digirep@iastate.edu).

OPERATING CHARACTERISTICS OF A URANIUM GRAPHITE  
SUBCRITICAL ASSEMBLY

by

Fred Hubbard Baughman

A Thesis Submitted to the  
Graduate Faculty in Partial Fulfillment of  
The Requirements for the Degree of  
MASTER OF SCIENCE

Major Subject: Engineering

Approved:

Signatures have been redacted for privacy

Iowa State College

1957



## TABLE OF CONTENTS

	Page
INTRODUCTION. . . . .	1
REVIEW OF THE LITERATURE. . . . .	2
THEORY OF THE SUBCRITICAL ASSEMBLY. . . . .	7
DESCRIPTION OF APPARATUS AND EXPERIMENTAL PROCEDURE .	11
DISCUSSION OF RESULTS . . . . .	19
CONCLUSIONS . . . . .	40
SUGGESTIONS FOR FURTHER STUDY . . . . .	42
LITERATURE CITED. . . . .	44
ACKNOWLEDGMENTS . . . . .	45
APPENDIX. . . . .	46

## INTRODUCTION

Today the subcritical assembly is a convenient tool of the nuclear scientist and engineer. It has several inherent advantages which make it particularly useful. It is much cheaper to assemble and operate than is a full scale reactor. The amounts of materials used are much less. It is inherently safe, no extensive shielding need be provided, and work can be carried on with none of the physical restrictions necessary near a reactor.

A natural uranium, graphite moderated subcritical assembly has been constructed recently at Iowa State College. This assembly will be useful in at least two capacities. First, it will provide extensive instructional opportunities, and the chance to compare classroom calculations with actual experimental results. Secondly, it will provide a research facility for numerous thesis investigations by graduate students.

Before other studies could be undertaken, it was necessary to develop safe and efficient procedures as well as to determine the basic operating characteristics of this assembly. It was with this purpose in mind that the present thesis was undertaken.



## REVIEW OF THE LITERATURE

The historical role played by the subcritical assembly in achieving the first self sustaining nuclear chain reaction has been given by Smyth (1). It is summarized below.

On December 2, 1942, mankind initiated his first self sustaining nuclear chain reaction at the University of Chicago (1, p. 70). This event marked the culmination of months of concentrated effort by many scientists and engineers. It could not have occurred as it did without the subcritical assembly leading the way.

By June 1940 it had been determined that the best possibility for a self sustaining chain reaction lay in the thermal neutron fission of  $U^{235}$ , using a heterogeneous mixture of graphite and natural uranium (1, p. 38). It was known that in the fission of  $U^{235}$  more than 2 fast neutrons were produced, on the average, for every neutron consumed in fission. However, most of these spare neutrons were absorbed by other materials in slowing down, or escaped altogether, and thus were lost before they in turn were able to react with other uranium nuclei to produce fission. The problem was to arrange the fissionable material and moderator in such a manner that enough of the neutrons were conserved to sustain a chain reaction.

Two main avenues of approach to this problem were possible. An elaborate series of investigations into the nuclear



properties of various materials was initiated, and theoretical calculations were begun based on these data. However, since speed was the controlling factor at that time, the major effort was directed into the empirical approach, and here the subcritical assembly became the primary means of investigating the problem.

The very small amounts of materials available, and the extreme costs involved, made full scale experiments impossible. The method used then was to construct a pile of about one fourth to one third the size believed necessary for criticality.

From the results of experiments conducted with such a subcritical assembly it was possible to predict the characteristics of a similar full scale reactor.

Since such a subcritical assembly could not sustain a chain reaction an external source of neutrons was placed near the bottom of the structure. The flux distribution in such an assembly then decreased exponentially with distance from the external source. This fact led to the subcritical assembly being called the "exponential pile".

Doctors Fermi and Szilard had suggested the use of graphite as a moderator for a chain reaction. Further, it was they who developed the lattice structure, in which lumps of uranium would be placed at regular intervals in a matrix of graphite (1, p. 23). This lattice structure had definite advantages over a uniform mixture of uranium and moderator.



In July 1941 the first subcritical assembly was set up at Columbia University. It was a graphite cube 8 ft. on a side, containing approximately 7 tons of uranium oxide distributed in lumps throughout the graphite. An external radium-beryllium neutron source was placed near the bottom of the assembly. Similar structures were set up in September and October of 1941. The multiplication factor,  $k$ , and the infinite multiplication factor,  $k_{\infty}$ , were computed in each case. For the third assembly,  $k_{\infty}$  reached 0.87 (1, p. 42). The problem remaining was to get  $k_{\infty}$  to reach or surpass 1.00 by using purer materials and possibly by using different lattice arrangements.

Within the following year a series of experiments was conducted using subcritical assemblies. In each experiment the uranium-graphite ratio was varied, oxides of improved purities were used, lattice spacing was varied, and various sizes and shapes of fuel lumps were tried. The ninth pile of this series was constructed in July 1942. The graphite used in this case was sufficiently free of impurities that it absorbed 20 per cent less neutrons than the best previously available commercial graphite. Calculations based on this assembly showed that for a reactor of infinite size,  $k = 1.007$ . An infinite multiplication factor greater than 1.00 had been reached (1, p. 69), and the subcritical assembly had been the means of achieving this goal.

Since 1942 the subcritical assembly has been used



extensively in developing new reactor types and in studying associated problems. At the Hanford Atomic Products Operation over 100 subcritical experiments have been conducted (2, p. 309). These experiments have had as their objective the finding of a better water-cooled graphite lattice for plutonium production and providing improved knowledge of lattice theory.

Argonne National Laboratory has been conducting a series of fast exponential experiments (2, p. 342). This series of experiments was designed to obtain fundamental information about the physics of dilute fast reactors. In connection with the School of Nuclear Science and Engineering, Argonne National Laboratory also operates a graphite moderated natural uranium subcritical assembly as well as a heavy water moderated natural uranium assembly.

In order to aid in the design of liquid metal cooled reactors, North American Aviation has conducted a series of subcritical experiments with a simulated sodium coolant (2, p. 309). These experiments included both natural and enriched uranium fuel elements in a graphite moderator. North American Aviation has also conducted a series of subcritical experiments to investigate the basic physics of a heavy water moderated lattice using various fuel enrichments (2, p. 268).

Beginning in 1944 and 1945 a series of subcritical experiments was conducted at the Oak Ridge National Laboratory. The purpose of these experiments was to determine values of buckling and other related characteristics for



Various diameters of natural uranium fuel rods in combination with a series of different volume ratios of light water moderator to uranium (2, p. 183). At the present time the Oak Ridge School of Reactor Technology has a graphite moderated natural uranium subcritical assembly for use primarily as an instructional tool (3).

A unique application of the subcritical assembly was made during the construction of the Brookhaven reactor. During a two-month period the partially completed reactor was used for a series of subcritical measurements. The results of these measurements were used to determine critical buckling and other lattice constants for the full scale reactor (2, p. 305). Later a series of subcritical experiments was conducted at Brookhaven to investigate the characteristics of light water moderated reactors with slightly enriched fuel (2, p. 184).



## THEORY OF THE SUBCRITICAL ASSEMBLY

The flux distribution in a subcritical assembly does not satisfy the wave equation for a critical reactor. However, if the assembly is quite large the thermal neutron flux distribution at a distance from boundaries and from the source can be represented quite well by the equation

$$\nabla^2 \phi + B_M^2 \phi = 0 \quad (1) \quad (4, p. 281)$$

$B_M^2$  is the material buckling for the system under consideration. Although this equation is valid only for a homogeneous system, it may be used for a heterogeneous system without serious error. There will be localized irregularities, but Equation 1 will give the overall neutron distribution.

Material buckling is determined from measurements of the thermal neutron flux distribution throughout the subcritical assembly. The critical size of a reactor of the same composition and geometric configuration can then be determined by equating geometrical buckling to the material buckling determined above.

For the usual rectangular subcritical assembly Equation 1 is expressed as

$$\frac{\partial^2 \phi}{\partial x^2} + \frac{\partial^2 \phi}{\partial y^2} + \frac{\partial^2 \phi}{\partial z^2} + B_M^2 \phi = 0 \quad (2)$$

If  $x$ ,  $y$ , and  $z$  are considered to be separable variables, then

$$\phi = [X(x) Y(y) Z(z)] \quad (3)$$



and Equation 2 becomes

$$\frac{1}{X} \frac{d^2 X}{dx^2} + \frac{1}{Y} \frac{d^2 Y}{dy^2} + \frac{1}{Z} \frac{d^2 Z}{dz^2} + B_M^2 = 0 \quad (4)$$

Letting

$$\frac{1}{X} \frac{d^2 X}{dx^2} = -\alpha^2 \quad (5)$$

$$\frac{1}{Y} \frac{d^2 Y}{dy^2} = -\beta^2 \quad (6)$$

$$\frac{1}{Z} \frac{d^2 Z}{dz^2} = +\gamma^2 \quad (7)$$

Equation 4 can be written

$$\alpha^2 + \beta^2 - \gamma^2 = B_M^2 \quad (8)$$

If the origin of the coordinate system is assumed to be at the center of the side of the assembly nearest the external neutron source, the boundary conditions can be expressed as:

1. The thermal neutron flux due to the external source of fast neutrons equals a constant,  $\phi_0$ , over the entire plane  $z = 0$ , and
2. Thermal neutron flux  $\phi = 0$  at  $x = \pm a/2$ ,  $y = \pm b/2$ , and  $z = c$ . ( $a$ ,  $b$ , and  $c$  are overall dimensions of the assembly, including extrapolation distance.)

For any given value of  $z$ , the flux is a maximum at  $x = 0$ ,  $y = 0$ , and is symmetrically distributed. It then follows that

$$X_m = A_m \cos\left(\frac{m\pi x}{a}\right) \quad (9)$$

$$Y_n = C_n \cos\left(\frac{n\pi y}{b}\right) \quad (10)$$



$$\alpha^2 = \left(\frac{m\pi}{a}\right)^2 \quad (11)$$

$$\text{and } \beta^2 = \left(\frac{n\pi}{b}\right)^2 \quad (12)$$

Substituting in Equation 8 leads to the form

$$\gamma_{mn}^2 = \left(\frac{m\pi}{a}\right)^2 + \left(\frac{n\pi}{b}\right)^2 - B_M^2 \quad (13)$$

The solution for  $Z$  is of the form  $Z(z) = F \sinh \gamma(c - z)$ , and the general solution may be expressed as

$$Z_{mn} = F_{mn} \sinh \gamma_{mn}(c - z) \quad (14)$$

Combining Equations 9, 10 and 14, the general solution of the wave equation becomes

$$\phi(x, y, z) = \sum_{m=1}^{\infty} \sum_{n=1}^{\infty} A'_{mn} \cos\left(\frac{m\pi x}{a}\right) \cos\left(\frac{n\pi y}{b}\right) \sinh \gamma_{mn}(c - z) \quad (15)$$

where  $A_m$ ,  $C_n$ , and  $F_{mn}$  are combined into  $A'_{mn}$ .

If the external neutron source is at least two slowing down lengths below the  $z = 0$  plane, then it can be assumed that virtually all neutrons have been thermalized by the time they enter the subcritical assembly. Under those conditions the only term of Equation 15 that is of any significance is the fundamental mode ( $m = 1$ ,  $n = 1$ ). Equation 15 then reduces to

$$\phi = A_{11} \cos \frac{\pi x}{a} \cos \frac{\pi y}{b} \sinh \gamma(c - z) \quad (16)$$

$$\phi(z) = F \sinh \gamma(c - z) = F' [e^{\gamma(c-z)} - e^{-\gamma(c-z)}] \quad (17)$$

This can be further reduced to



$$\phi(z) = F' e^{\gamma c} \left[ e^{-\gamma z} - e^{-2\gamma c} e^{\gamma z} \right] \quad (18)$$

For given physical dimensions,  $e^{\gamma c}$  is a constant, and Equation 18 becomes

$$\phi(z) = C' e^{-\gamma z} \left[ 1 - e^{-2\gamma(c-z)} \right] \quad (19)$$

If the vertical dimension,  $c$ , is very large, and if  $z$  is not allowed to approach  $c$ , then  $\left[ 1 - e^{-2\gamma(c-z)} \right]$  approaches unity. Equation 19 simplifies to

$$\phi(z) = C' e^{-\gamma z} \quad (20)$$

Equation 20 indicates that the thermal neutron flux distribution decreases exponentially with increasing  $z$ . Thus a plot of distance  $z$  versus the natural logarithm of the flux (or of a quantity proportional to flux) should be a straight line of slope  $\gamma$ . Near the top of the assembly the points will deviate from a straight line due to neglecting the end correction term  $\left[ 1 - e^{-2\gamma(c-z)} \right]$  in Equation 20.

The slope,  $\gamma$ , is really  $\gamma_{11}$ , and Equation 13 can be written

$$\left( \frac{\pi}{a} \right)^2 + \left( \frac{\pi}{b} \right)^2 - \gamma^2 = B_M^2 \quad (21)$$

This equation can be solved for material buckling, all other quantities now being known. By setting this value of material buckling equal to geometrical buckling, the critical size of the full scale counterpart of the subcritical assembly can be determined.



## DESCRIPTION OF APPARATUS AND EXPERIMENTAL PROCEDURE

Figure 1 is an overall view of the subcritical assembly. Figure 2 shows important dimensions and the arrangement and numbering of the foil slots. The assembly consists of cylinders of reactor grade graphite 60 in. long and 7 in. in diameter. These cylinders had the sides cut flat to form squares 6 in. across with rounded corners. These are stacked in a square lattice, ten rows wide and fourteen rows high. The top five rows are only 5 in. high by 6 in. wide, making the overall dimensions of the assembly 60 by 60 by 79 in. high.

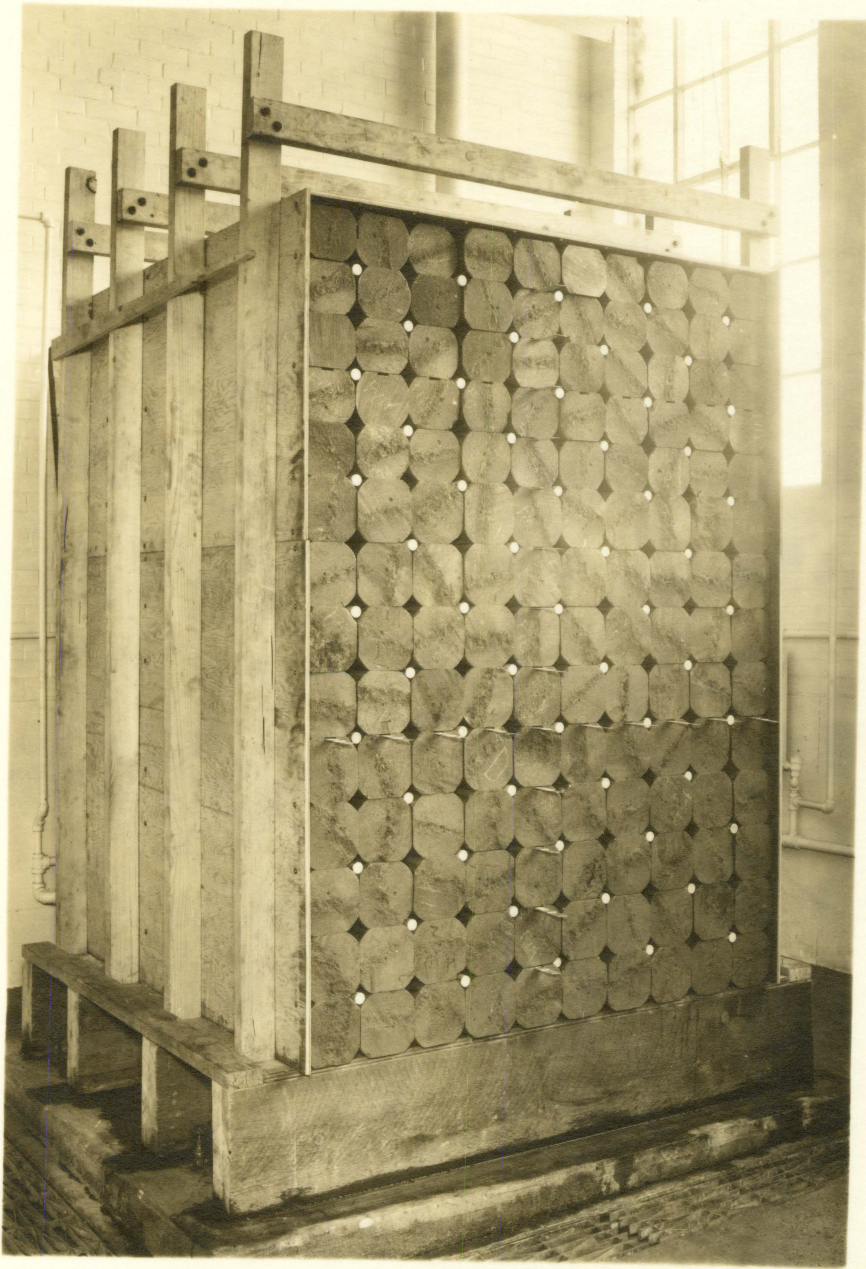
This pile is set on a wooden base, and an external neutron source is centered under it. Water filled aluminum tanks entirely surround the external neutron source, providing adequate shielding against both gamma and neutron radiation.

The rounded corners between the graphite blocks present 117 holes approximately  $1\frac{1}{2}$  in. across for insertion of fuel elements. The spacing of these holes allows a minimum fuel lattice of 6 in. when all holes are filled. By removing alternate fuel elements, or entire rows of fuel elements, the lattice spacing may be varied from 6 in. to 8.5 in. (8.484 in.), 12 in. or larger if desired.

Thirty-one small horizontal slots pierce the assembly from the east face (Figure 2). These slots provide for the

Figure 1. Subcritical assembly







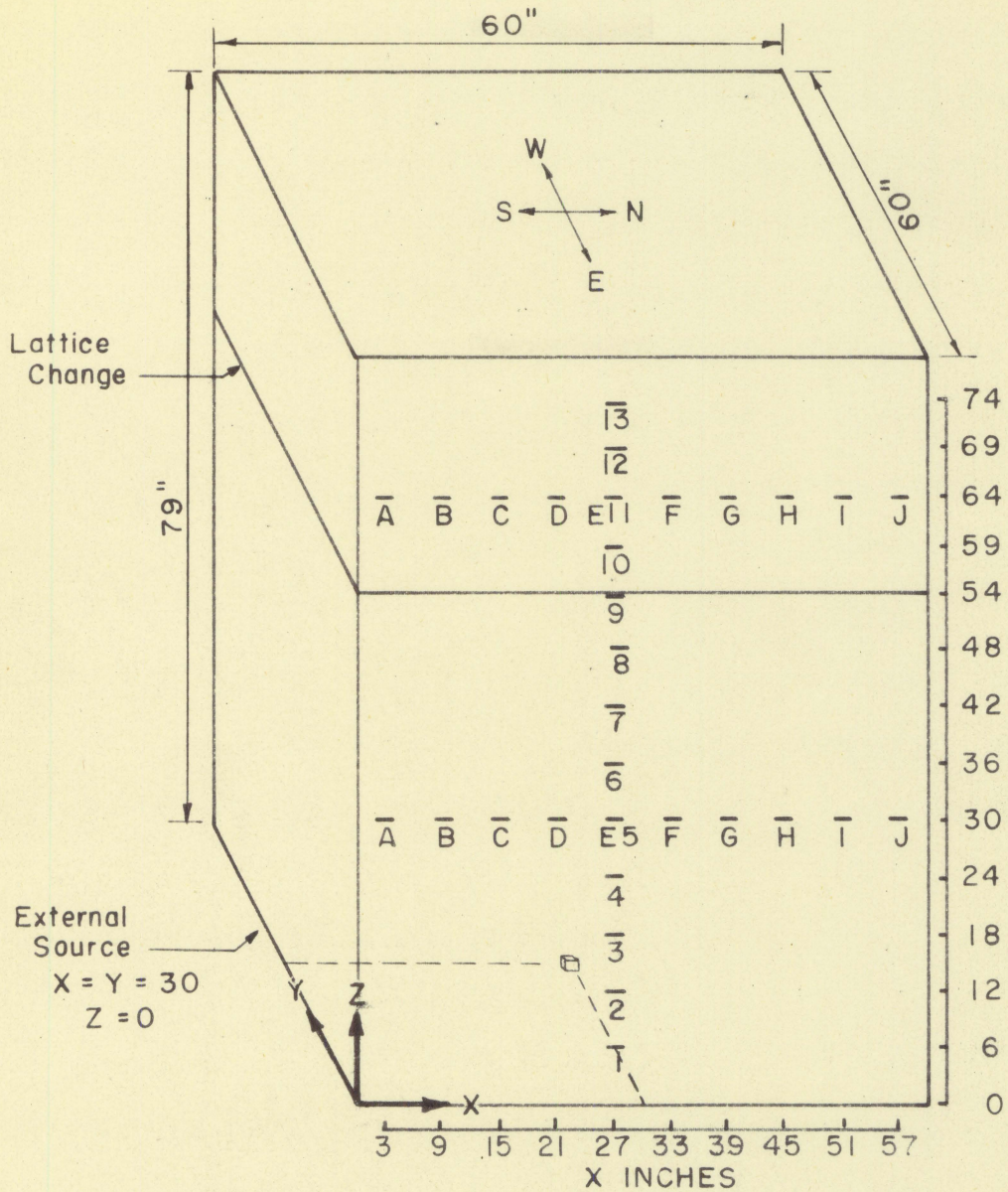


Figure 2. Subcritical assembly - dimensions and foil holder arrangement



irradiation of indium foils to use in determining the neutron flux at various points throughout the pile. One vertical hole is available for possible simulation of control rod effects. All vertical sides and the top of the assembly are covered with 0.010 in. sheet cadmium to present essentially a "black boundary" to neutrons.

The indium foils used in this experiment are 1.00 in. by 1.50 in. by 0.003 in. thick. They are mounted on aluminum planchets with DuPont "Duco" cement, each with the weight and foil number inscribed on the back. The average weight of the 160 foils in use is 0.5943 grams. Aluminum foil holders allow placing of the foils in the previously described slots at 3 in. center to center spacing across the assembly. For measuring fast neutron flux indium foils can be wrapped in 0.010 in. cadmium sheet.

Foil counting apparatus consists of a suitable decimal scalar and either a mica end window Geiger-Mueller counter or a thin glass wall Geiger-Mueller counter.

The use of indium foils to measure neutron fluxes makes use of the so-called activation method. In this method the indium is exposed in the neutron flux. Indium has a high cross section for thermal neutrons and becomes radioactive, emitting a beta particle with a 54 min. half life. The neutrons are quite difficult to measure directly, but the beta activity of the indium is proportional to the neutron



activity, and beta particles can be detected and counted quite readily.

For each experimental run indium foils were placed in the assembly and irradiated for a minimum of 5.4 hr. or six half lives; in most cases the irradiation time was much longer than this. This procedure insured an activity of at least 98.4 per cent of maximum of the 54 min. activity. Foils were then removed individually or in groups of not more than eight, depending upon the particular experiment. The foils were counted in a nearby room having a much lower background than the room containing the subcritical assembly. Each foil was counted for 3 min. Then these counts, less background, were corrected back to the time of removal from the assembly to give net activity in counts per minute. In each instance in which more than one foil was removed for counting at a given time the foil expected to have the least activity was counted first. This helped to minimize distortion of low counting rates by large corrections to time of removal. No foil was counted sooner than 3 min. after removal from the assembly. This allowed a 13 sec. indium activity to decay to less than 0.01 per cent, and only the 54 min. beta activity remained.

The majority of the data in this set of experiments was obtained using a 100 millicurie radium-beryllium external neutron source. This was the largest source available at the time the experiments were begun. Five, 1 curie



plutonium-beryllium sources became available later, and two sets of data were obtained using this larger neutron source.

The first experimental arrangement consisted of the 6 in. lattice spacing with the 100 millicurie neutron source. A complete survey of the lower horizontal row of foils plus the entire vertical row of foils was taken in this configuration. Foils were spaced at 6 in. intervals from the east face to the centerline of the assembly. Next a vertical survey was made using cadmium covered center line foils to determine the cadmium ratio. The third set of data was obtained with the same 6 in. lattice, but with only the 22 center line foils loaded. This was to investigate the extent of flux depression caused by the 132 foils of the original loading.

The lattice spacing was then changed to 8.5 in. and with all foils loaded only the 18 in. and 30 in. (center line) foils were counted. A set of foils was also placed completely through the assembly in the y direction. Data obtained from these foils were used in determining any flux variation due to the unsymmetrical foil loading employed.

Fuel loading was changed again, and the 18 in. and 30 in. flux measurements were repeated with a 12 in. lattice spacing.

The 100 millicurie radium-beryllium neutron source was replaced by a cluster of five, 1 curie plutonium-beryllium neutron sources. Two further experimental runs were conducted. First a survey was taken with all fuel elements



removed. These data were used in determining the effect of subcritical multiplication. Finally, a set of data was collected using the 8.5 in. lattice with the larger neutron source. These data provided a correlation for the 8.5 in. lattice between characteristics obtained with the small external neutron source and characteristics obtained with the large external neutron source. Again one row of foils was extended entirely through the assembly to investigate the symmetry in the y direction.

The indium foils were positioned in a holder approximately 0.20 in. from the end window Geiger-Mueller tube in a constant position relative to the tube. In each case the area of the foil was greater than the area subtended by the end window tube, and no correction was made for weight variations due to the slight area variations among the foils.

A strontium-yttrium sample was used as a standard source, and this sample was counted at least once during each run. This procedure was followed to insure that no change in the experimental arrangement or deviation in the Geiger-Mueller tube characteristics would creep in undetected and invalidate the correlation between data obtained on different occasions.



## DISCUSSION OF RESULTS

The results of this series of flux measurements are presented graphically as Figures 3 through 14. The data on which these figures are based are tabulated in the Appendix. In a number of the figures a horizontal flux distribution is plotted. Since the theoretical flux distribution has the shape of a cosine curve, cosine curves were faired through the experimental points rather than attempting to fit some other smooth curve to the points.

A detailed survey was made with the 6 in. lattice and the small external neutron source. Due to the small activity of this source, counting rates were quite low and standard deviations were necessarily large. Extended counting periods would have lowered deviations, but this was not practical due to the excessive decay of the 54 min. beta activity while counting over a longer period. Figure 3 displays the flux distribution in the x direction as compared to the theoretical cosine distribution. Vertical height of the symbols indicates standard deviation. It is noted that the scatter of experimental points decreases and the flux distribution conforms more closely to the plotted cosine curves as y increases toward the center line of the assembly.

It was desired to determine whether a large number of indium foils present in the assembly produced a measurable effect on the overall flux level. Figure 4 shows that any



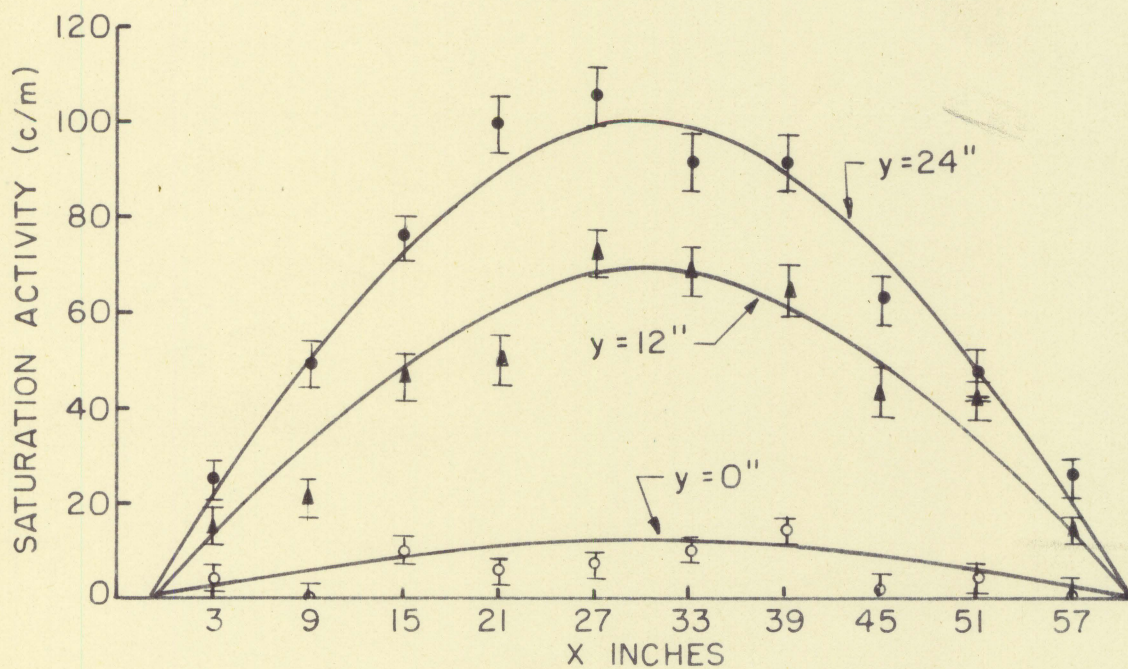
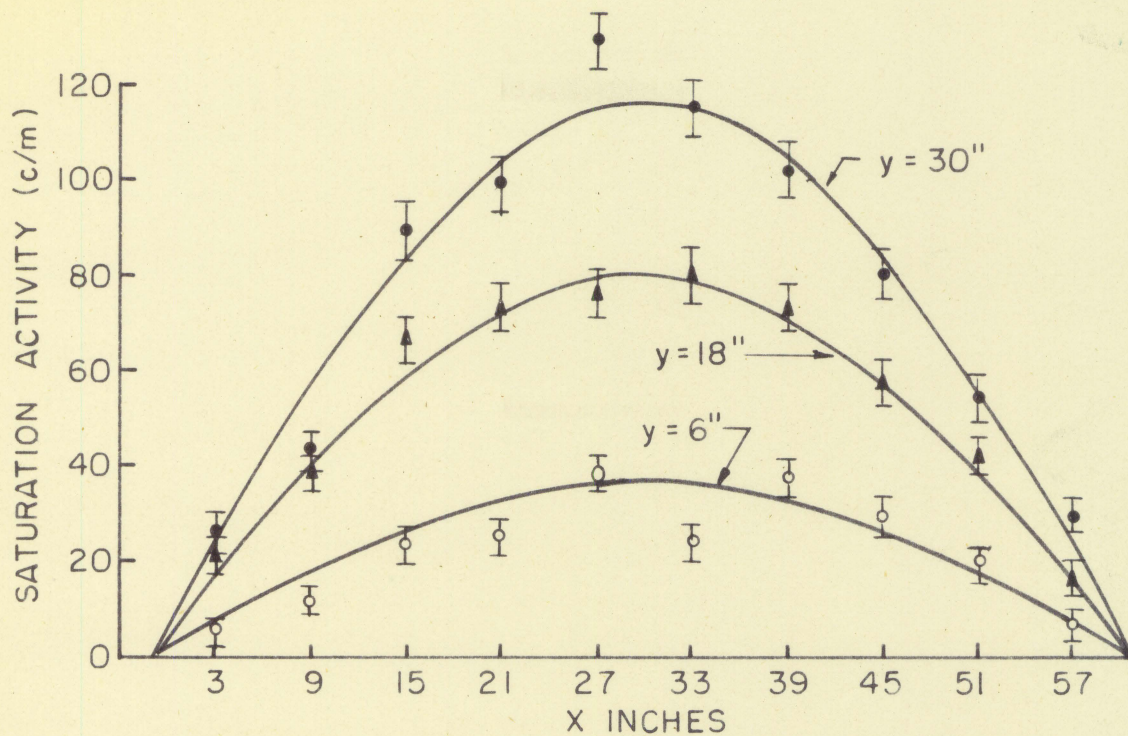


Figure 3. Horizontal flux survey, 6 inch lattice,  
z = 30 inches



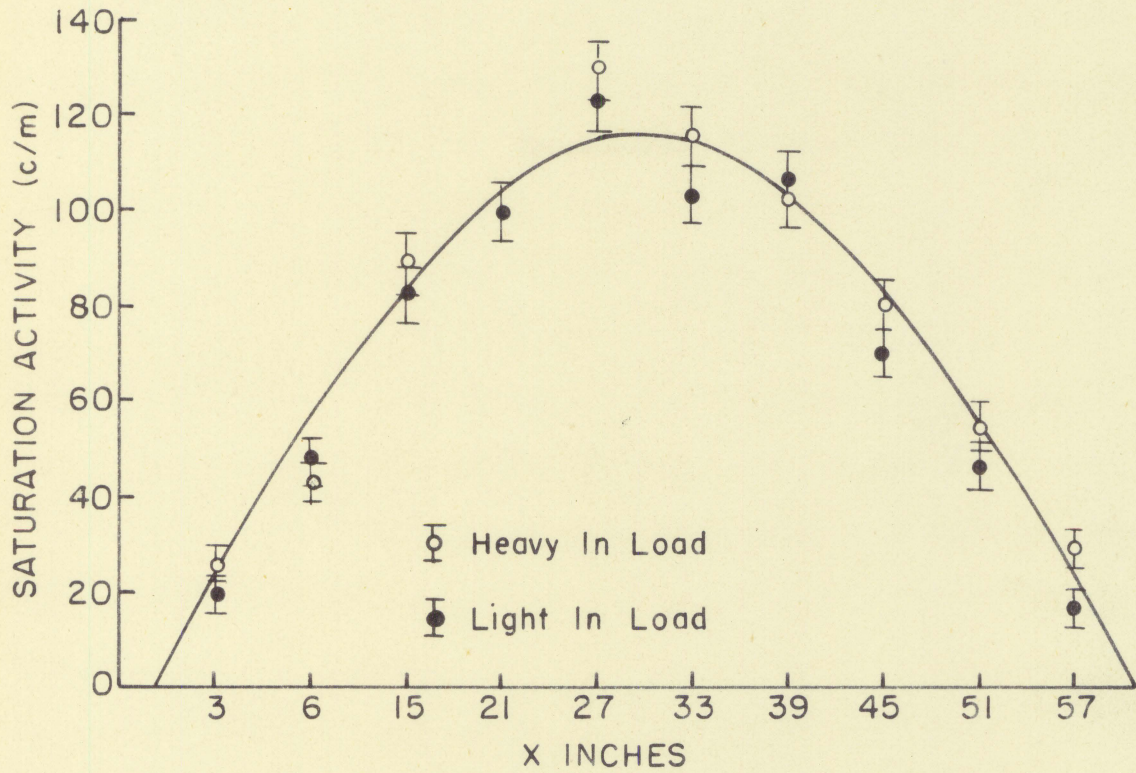


Figure 4. Horizontal flux survey for light and heavy indium loads,  $y = 30$  inches,  $z = 30$  inches



variation due to foil loading is within the limits of normal scattering, and only one cosine curve is plotted through both sets of experimental points. This conclusion is also supported by the data of Figure 8. Figure 8 illustrates the symmetry in the y direction even though many more foils were placed in the east half of the assembly than in the west half.

In order to determine the degree to which the fast source neutrons had been thermalized, a vertical flux survey was made using cadmium covered indium foils. Figure 5 displays these data contrasted with the comparable data obtained with bare indium foils. A constant ratio of these two fluxes would indicate that all of the fast source neutrons had been thermalized (4, p. 124). The data indicate that fast neutrons still remain for some distance up from the bottom of the assembly. The apparently changing ratio near the top may be due to statistical scattering of the points because of the very low counting rates involved. It is believed that further investigation using the large external neutron source would show this trend to be in error.

Figure 6 compares the flux obtained with each of three lattice spacings. The 8.5 in. lattice gives the highest flux levels of the three lattices investigated. Some of the data obtained with the 12 in. lattice is believed to be in error, as these were the last counts made before an equipment failure. Since the nature of the failure was such that the counting rate became extremely high just before complete failure,



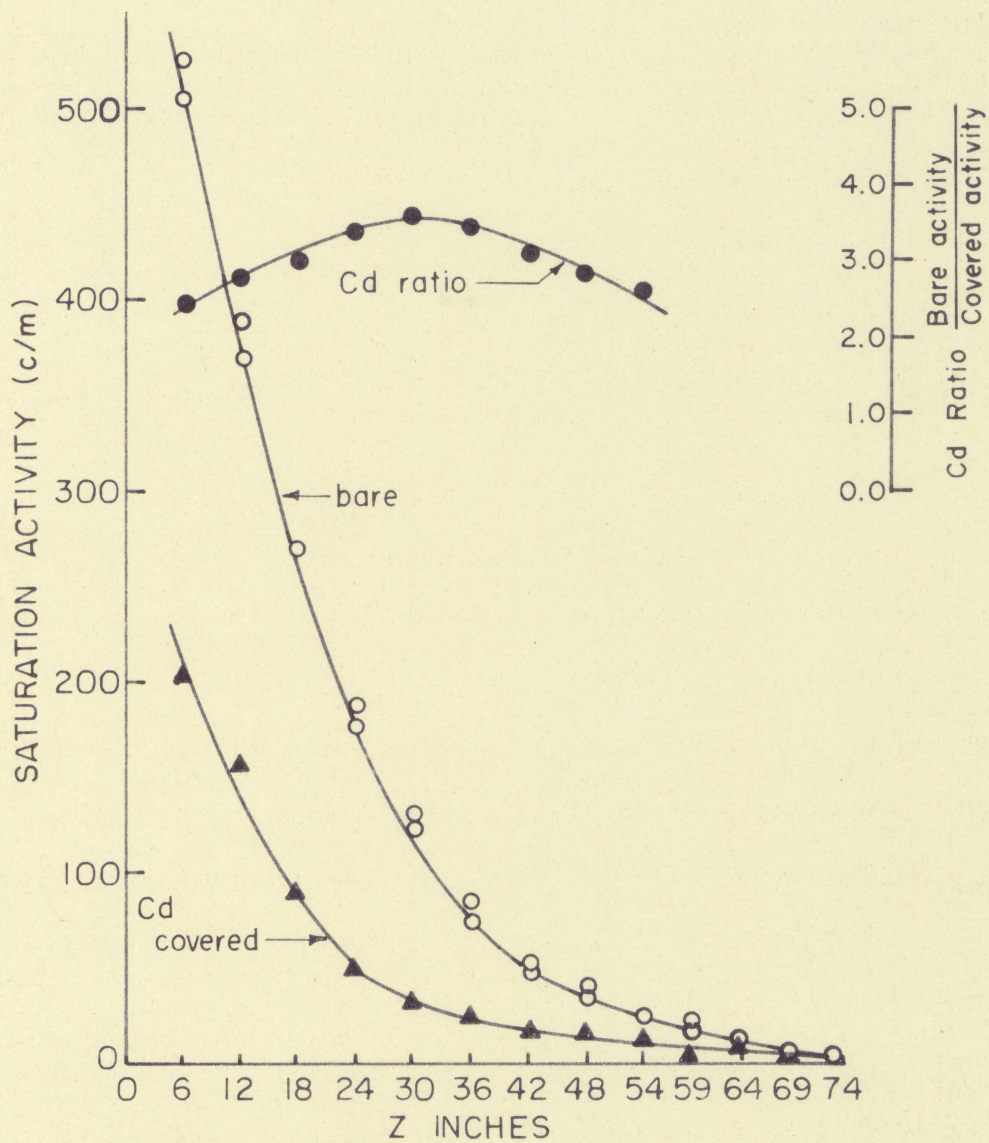


Figure 5. Cadmium ratio - 6 inch lattice,  $x = 27$  inches,  $y = 30$  inches



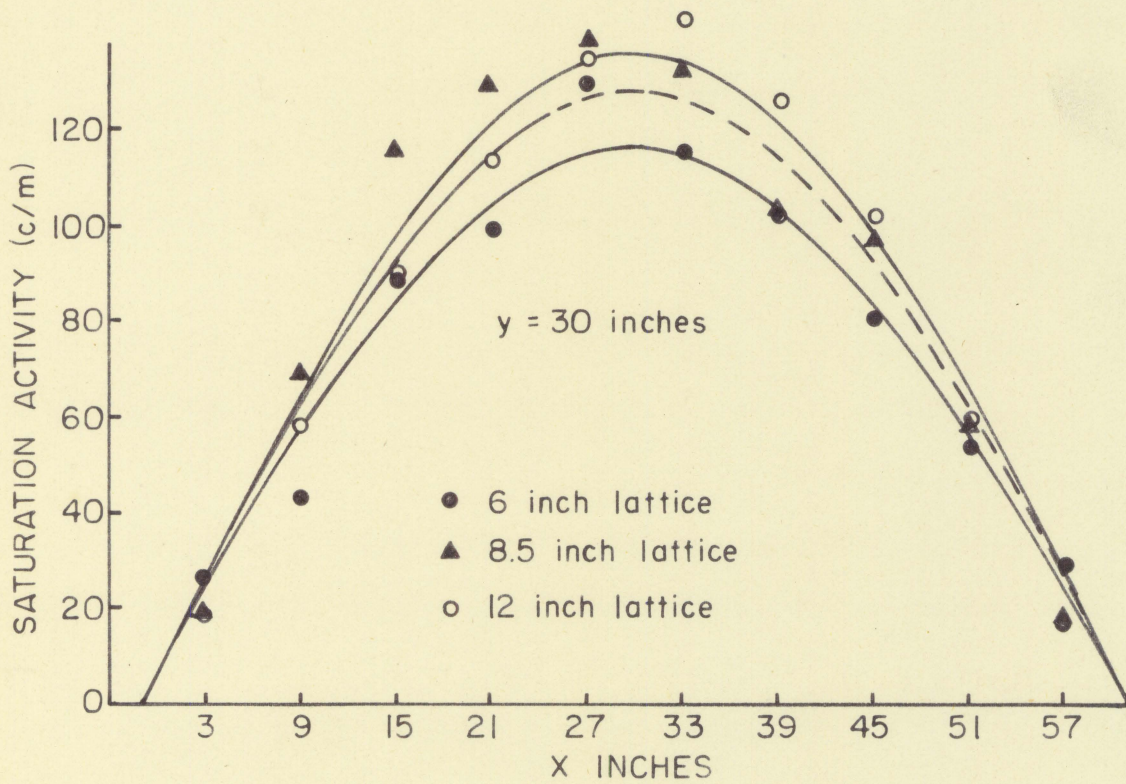
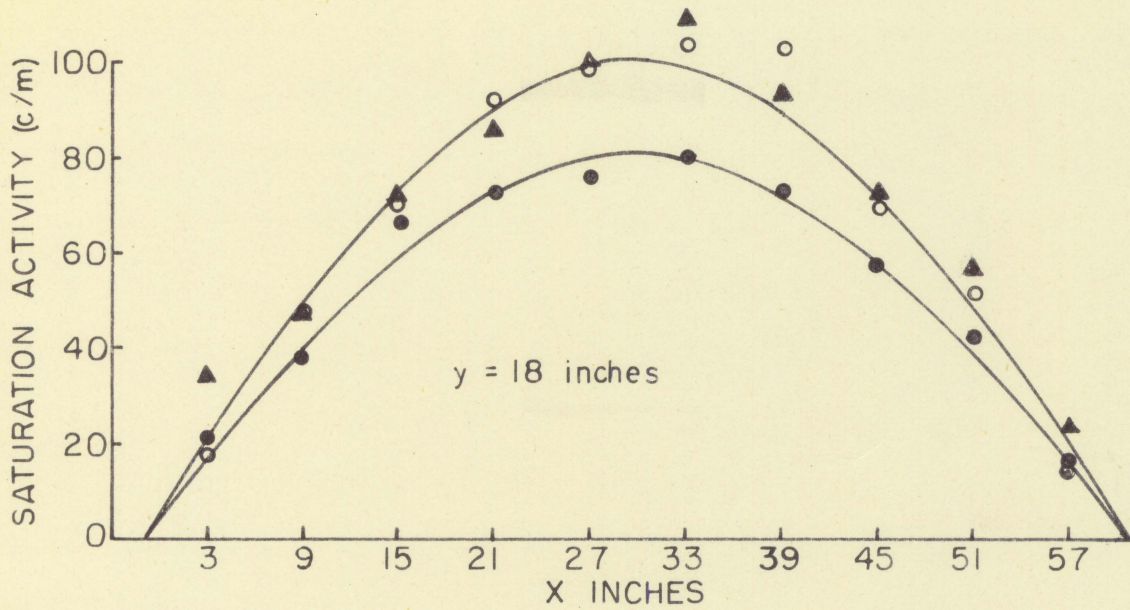


Figure 6. Lattice comparison - horizontal,  $z = 30$  inches



these experimental points are believed to indicate an unreasonably high flux. Therefore, the experimental points at  $x = 27$  in. and greater were disregarded. Instead, the cosine curve was fitted to points for  $x$  less than 27 in., and the curve drawn symmetrically. The dashed line indicates the extrapolated portion of the curve.

Prior to the completion of all experimental determinations a larger neutron source became available. Some data were obtained using this larger source with the 8.5 in. lattice. These results are presented both to confirm the findings obtained with the small neutron source and to demonstrate the great increase in flux levels obtained by use of a larger neutron source.

Figures 7 and 8 display the flux distribution in the  $x$  and  $y$  directions, respectively, with each of the neutron sources in place. In both cases the higher flux levels, corresponding to the larger neutron source, show little scatter of experimental points, excellent symmetry, and a good conformance to the theoretical cosine distribution. As has been noted previously, Figure 8 indicates no measurable deviation from the cosine flux distribution due to unsymmetrical indium foil loading in the  $y$  direction.

One set of data was obtained with all fuel elements removed from the assembly. The flux levels present under these conditions, when compared with the flux levels present



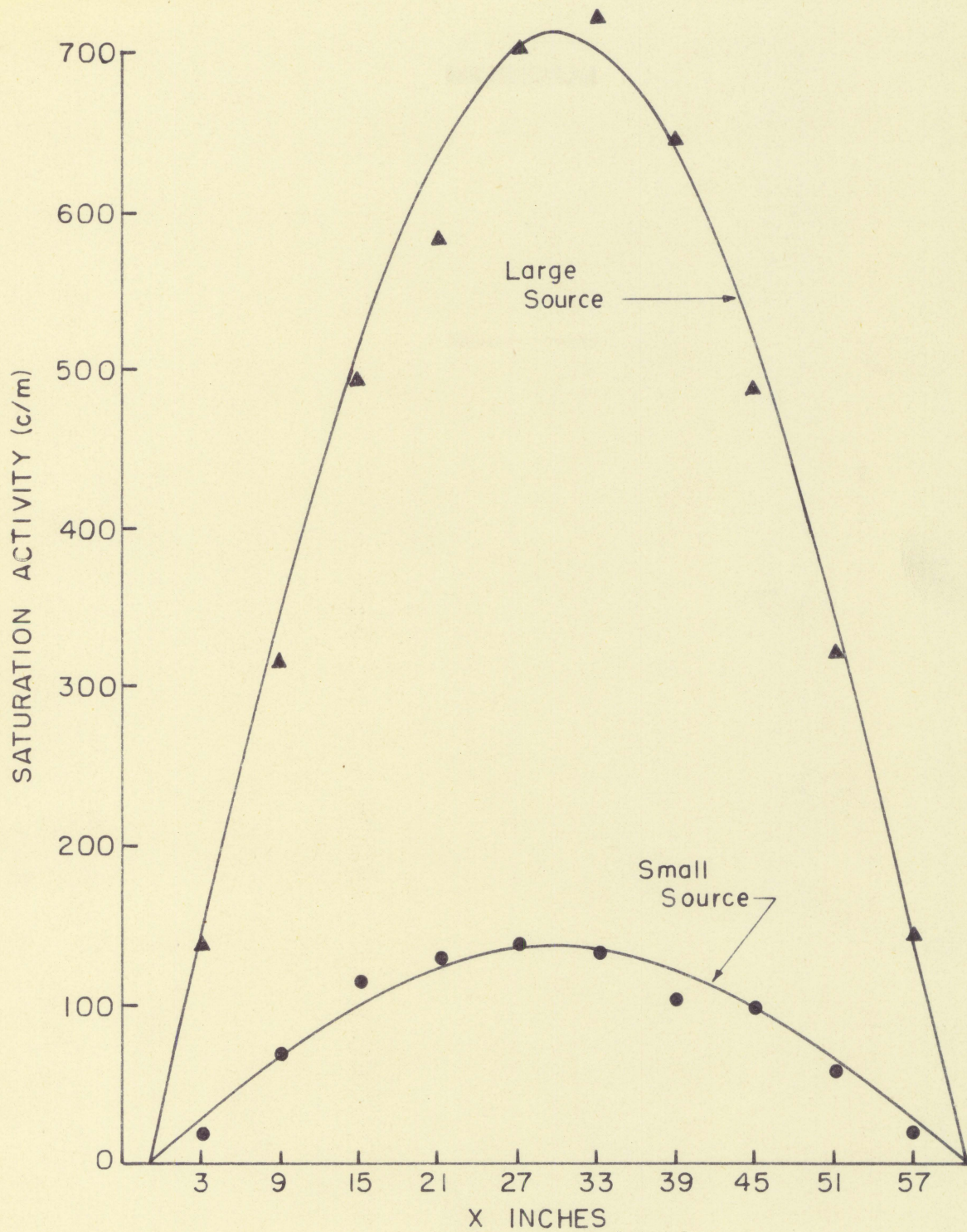


Figure 7. Horizontal flux survey, x direction, 8.5 inch lattice, different neutron sources



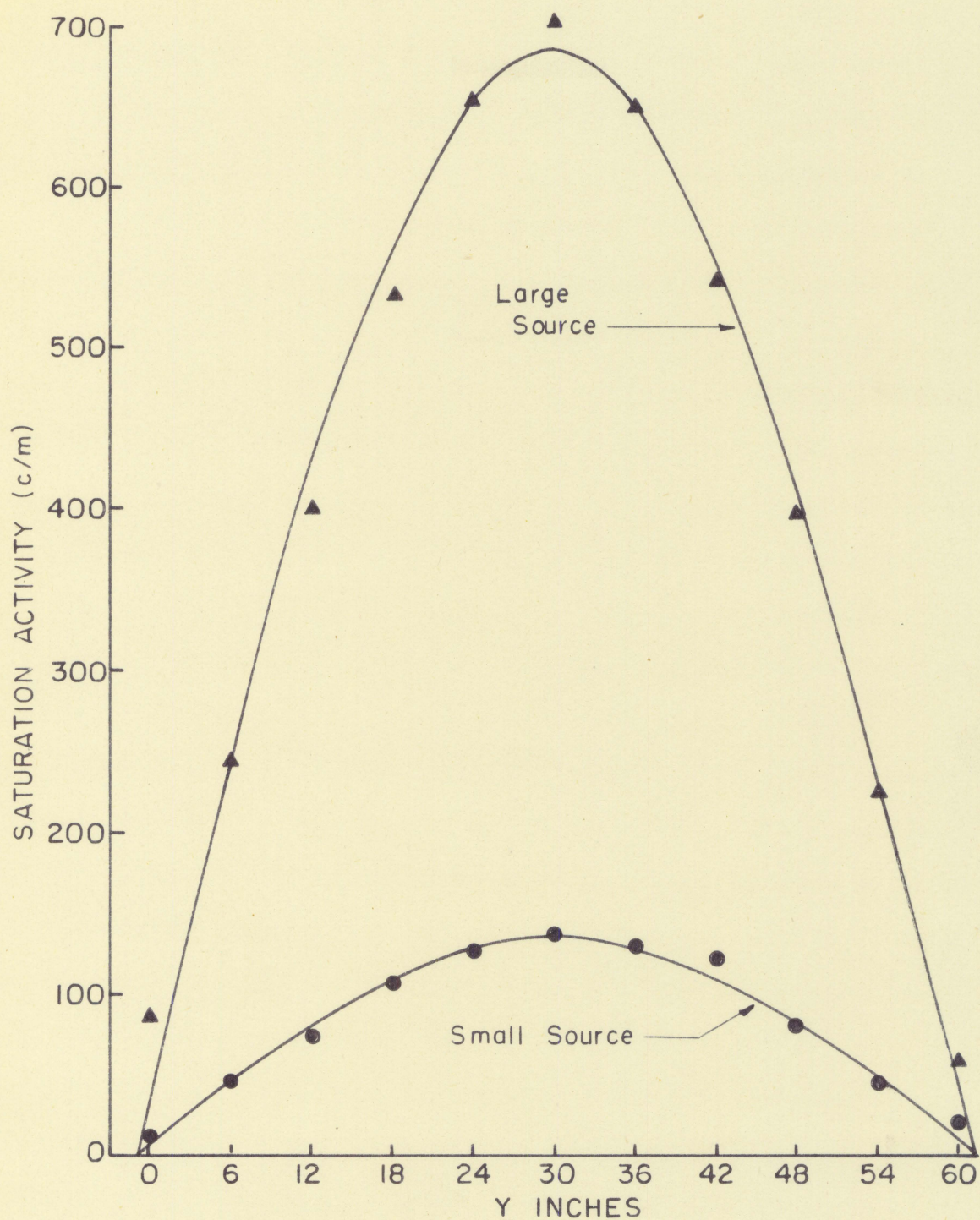


Figure 8. Horizontal flux survey, y direction, 8.5 inch lattice, different neutron sources



in the 8.5 in. lattice, indicate the effect of subcritical multiplication. Figure 9 shows that within 30 in. vertically of the base of the assembly the empty graphite lattice has a higher flux level than does the one with fuel elements in place. This is an indication that more neutrons are being absorbed by the fuel than are being produced by fission within the fuel. Above 30 in., however, the number of neutrons produced by fission in the uranium exceeds the number absorbed in the fuel, and the flux level with fuel elements in place is higher than the flux level of the empty assembly. Figure 10 compares the flux level at the 30 in. plane for various values of  $x$  horizontally. As stated above, the overall effect of the fuel elements is essentially zero at this distance from the base.

One of the most important characteristics which can be determined experimentally by means of a subcritical assembly is critical buckling. As developed previously, when flux (or a value proportional to flux) is plotted on a logarithmic scale versus distance from the external neutron source on a linear scale the slope of the line thus obtained is gamma. If the physical dimensions of the subcritical assembly are known, critical buckling can then be determined by using Equation 21.

In theory, critical buckling can be determined by first computing the infinite multiplication factor,  $k_{\infty}$ , and then solving the transcendental equation



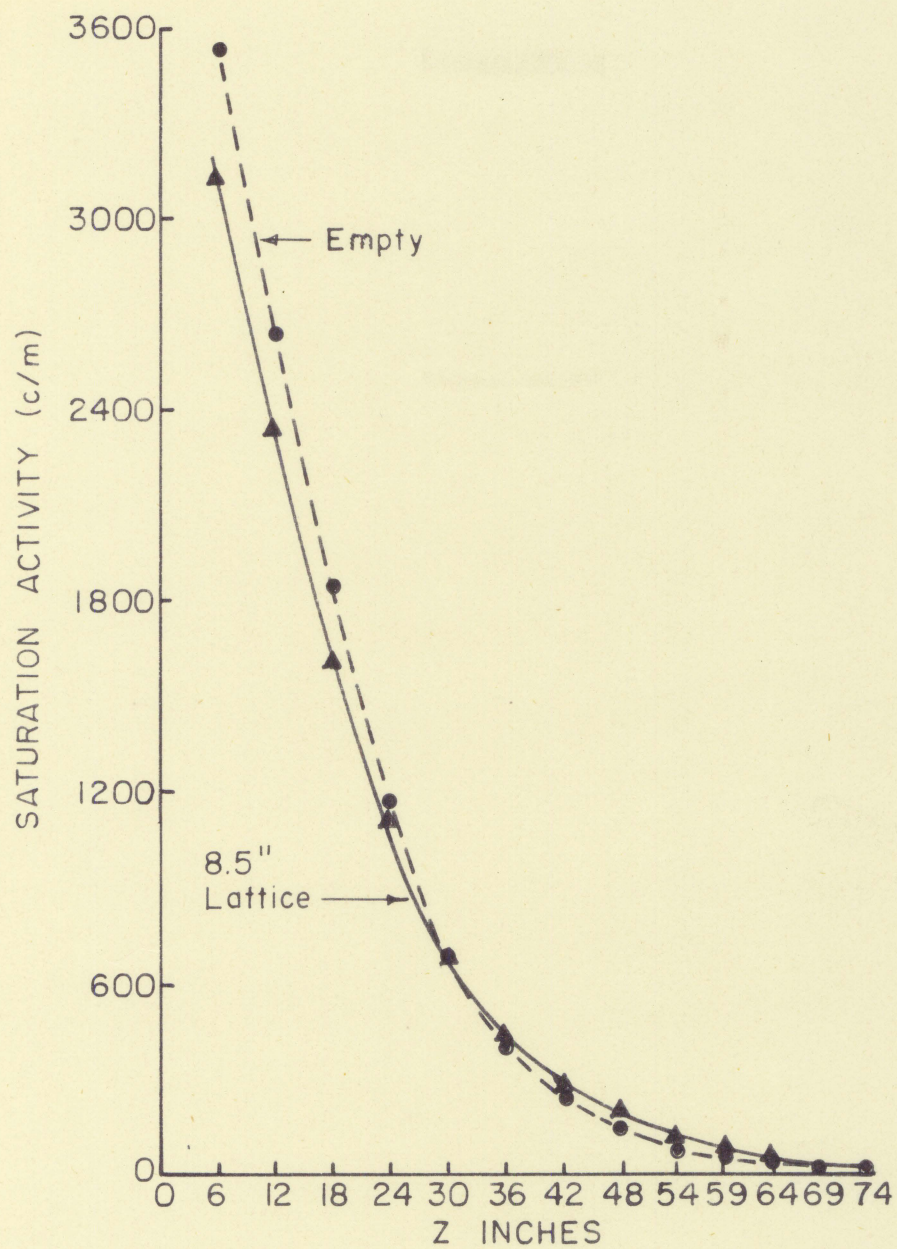


Figure 9. Effect of subcritical multiplication, 8.5 inch lattice,  $x = 27$  inches,  $y = 30$  inches



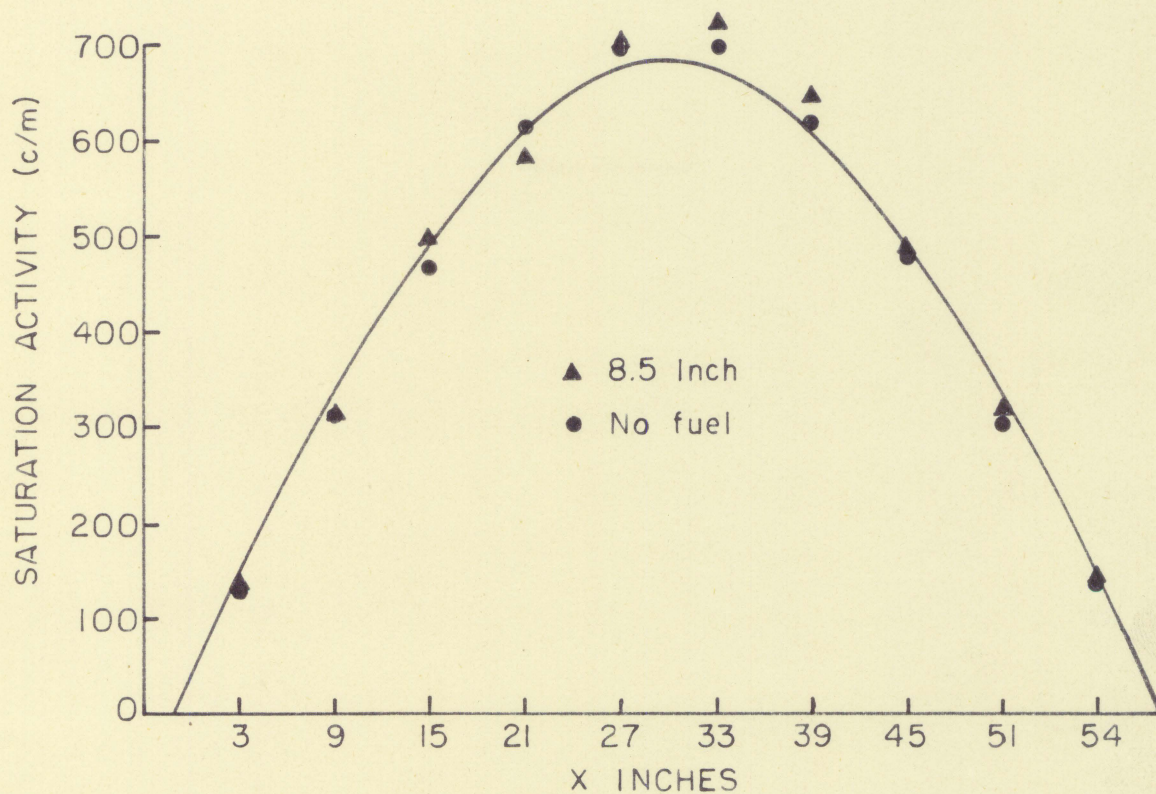


Figure 10. Effect of subcritical multiplication, 8.5 inch lattice,  $y = 30$  inches,  $z = 30$  inches



$$k_{\text{eff}} = 1 = \frac{k_{\infty} e^{-B^2 \tau}}{1 + L^2 B^2} \quad (22)$$

The infinite multiplication factor is computed from the four factor formula

$$k_{\infty} = \eta \epsilon p f \quad (23)$$

Computing  $\eta$  from the relation

$$\eta = \nu \frac{\sum f}{\sum_{\text{fuel}}} \quad (24)$$

gives a value for natural uranium fuel of  $\eta = 1.353$ . Cross sections used are those given by Kaplan (5, p. 490). From a figure given by Glasstone (6, p. 195), the fast fission factor,  $\epsilon$ , for the size fuel elements used in the subcritical assembly is 1.030. These two factors are independent of lattice spacing and remain the same for all three lattices.

The resonance escape probability,  $p$ , varies with the relative amounts of fuel and moderator present, and it is therefore different for each lattice spacing. The method of Glasstone (6, pp. 191-192) was used to determine  $p$ . Weights, volumes, and densities of fuel, cladding and graphite were determined from representative samples. The density of the graphite was computed to be 1.56 g/cm<sup>3</sup>. The overall dimensions of a fuel element were measured to be 8.40 in. long by 1.080 in. in diameter. Each fuel element weighed 2.018 kg, giving it an average density of 16.04 g/cm<sup>3</sup>. Each fuel element contained a rod of natural uranium 8.00 in. long and 1.00 in. in diameter. This left cladding of 0.040 in. thick



with 0.200 in. end plates. The density of the aluminum cladding and binder (assumed the same) was taken to be that of aluminum,  $2.71 \text{ g/cm}^3$ . The density of the uranium was then computed to be  $19.0 \text{ g/cm}^3$ .

Using these data, the square heterogeneous lattice was treated as a system of equivalent cylindrical unit cells (4, p. 265), and  $p$  was determined for each case.

The fourth factor, thermal utilization,  $f$ , also varies with lattice spacing. Thermal utilization was computed as shown by Murray (7, p. 87), and again the square lattice was treated as a system of equivalent cylindrical unit cells. Allowance was made for the presence of fuel, cladding, air space, and graphite moderator. For the size fuel element used, the disadvantage factor,  $F$ , was computed to be 1.0891.

Computed values of  $\eta$ ,  $\epsilon$ ,  $p$ ,  $f$ , and  $k_{\infty}$  are tabulated in Table 1.

Table 1. Theoretical calculation of critical buckling

Value	6 in. lattice	8.5 in. lattice	12 in. lattice
$\eta$	1.353	1.353	1.353
$\epsilon$	1.030	1.030	1.030
$p$	0.808	0.900	0.947
$f$	0.928	0.873	0.767
$k_{\infty}$	1.047	1.098	1.015
$B^2(\text{cm}^{-2})$	$83 \times 10^{-6}$	$137 \times 10^{-6}$	$15.5 \times 10^{-6}$



Having determined  $k_{\infty}$ , a first approximation for critical buckling can be obtained from Formula 25 which is valid for a large reactor

$$B^2 = \frac{k - 1}{M^2} = \frac{k - 1}{L^2 + \tau} \quad (25)(4, p. 216)$$

Fermi age,  $\tau$ , for graphite is 350 cm<sup>2</sup>. For a heterogeneous lattice, age may be taken as 10 per cent greater than that for the pure moderator (3, p. 201), giving a value of 385 cm<sup>2</sup>. Using values of  $f$  just computed,  $L^2$  was obtained from the formula

$$L^2 = L_0^2(1 - f) \quad (26)(4, p. 280)$$

Values of buckling obtained by Equation 25 were then substituted in the transcendental equation, Equation 22. The maximum error was 0.3 per cent. Slight adjustments gave values of buckling correct within 0.1 per cent.

The results of the above calculations for all three lattices are tabulated as Table 1.

The results of experimental determination are presented as Figures 11, 12, and 13. The bucklings computed from these figures are listed in Table 2.

In the interest of clarity, all buckling data have been displayed on a common figure. Figure 14 compares theoretical buckling from Table 1 with experimental values determined from Figures 11 through 13, as tabulated in Table 2.

Figure 11 compares vertical flux distribution for the three lattices at  $x = 27$  in. and  $y = 18$  in. No attempt was



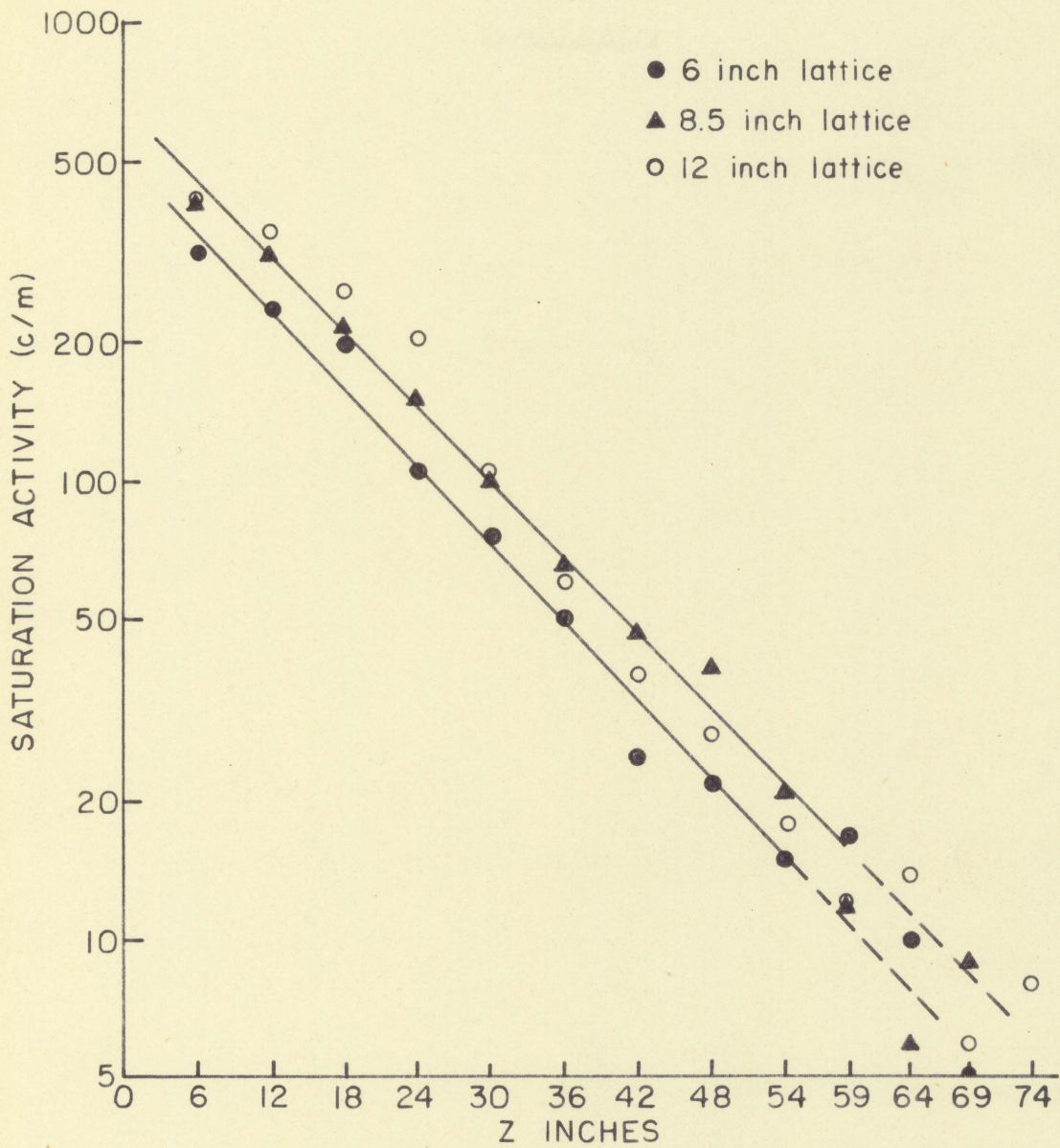


Figure 11. Lattice comparison - vertical,  $x = 27$  inches,  $y = 18$  inches



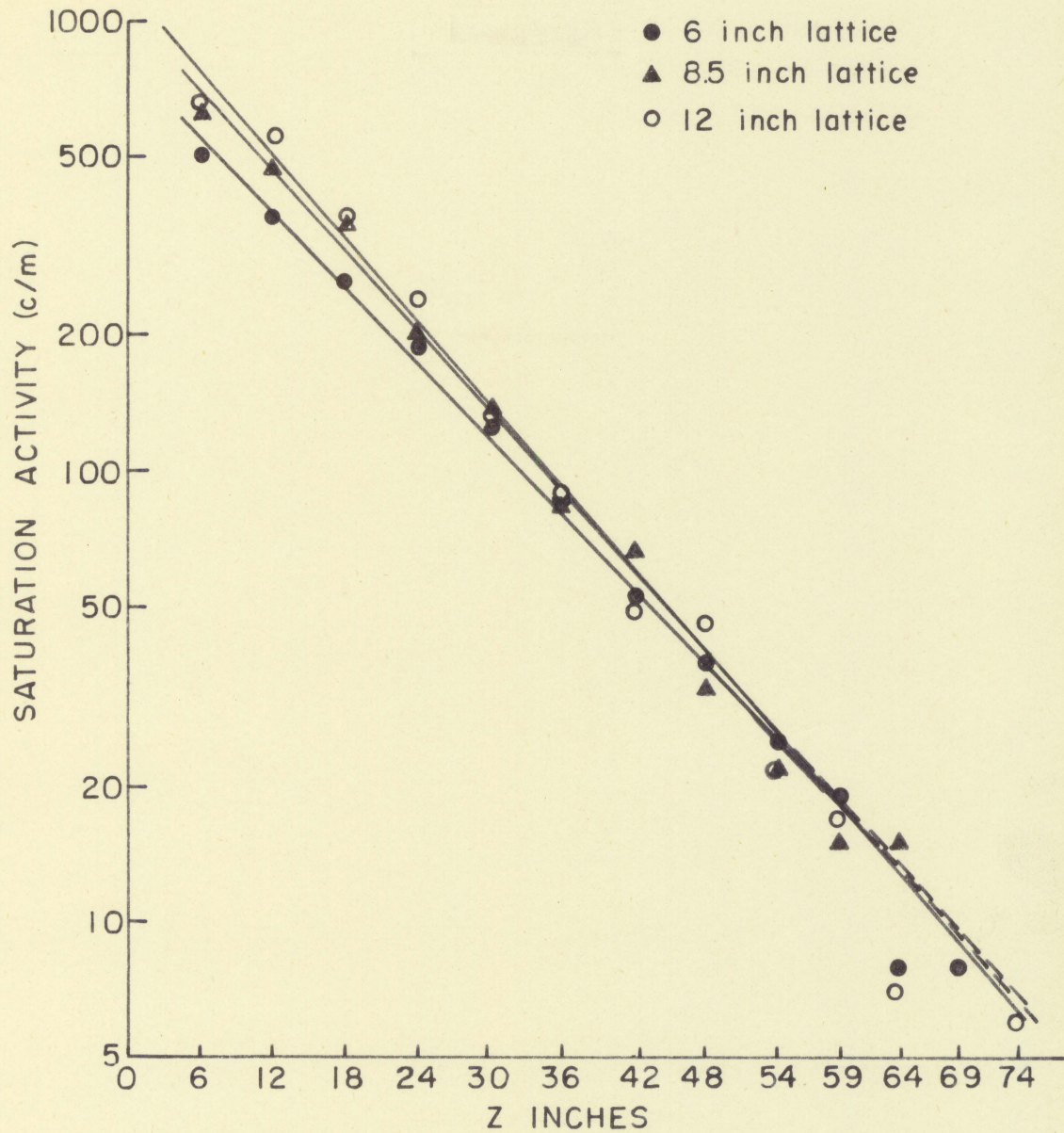


Figure 12. Lattice comparison - vertical,  $x = 27$  inches,  $y = 30$  inches



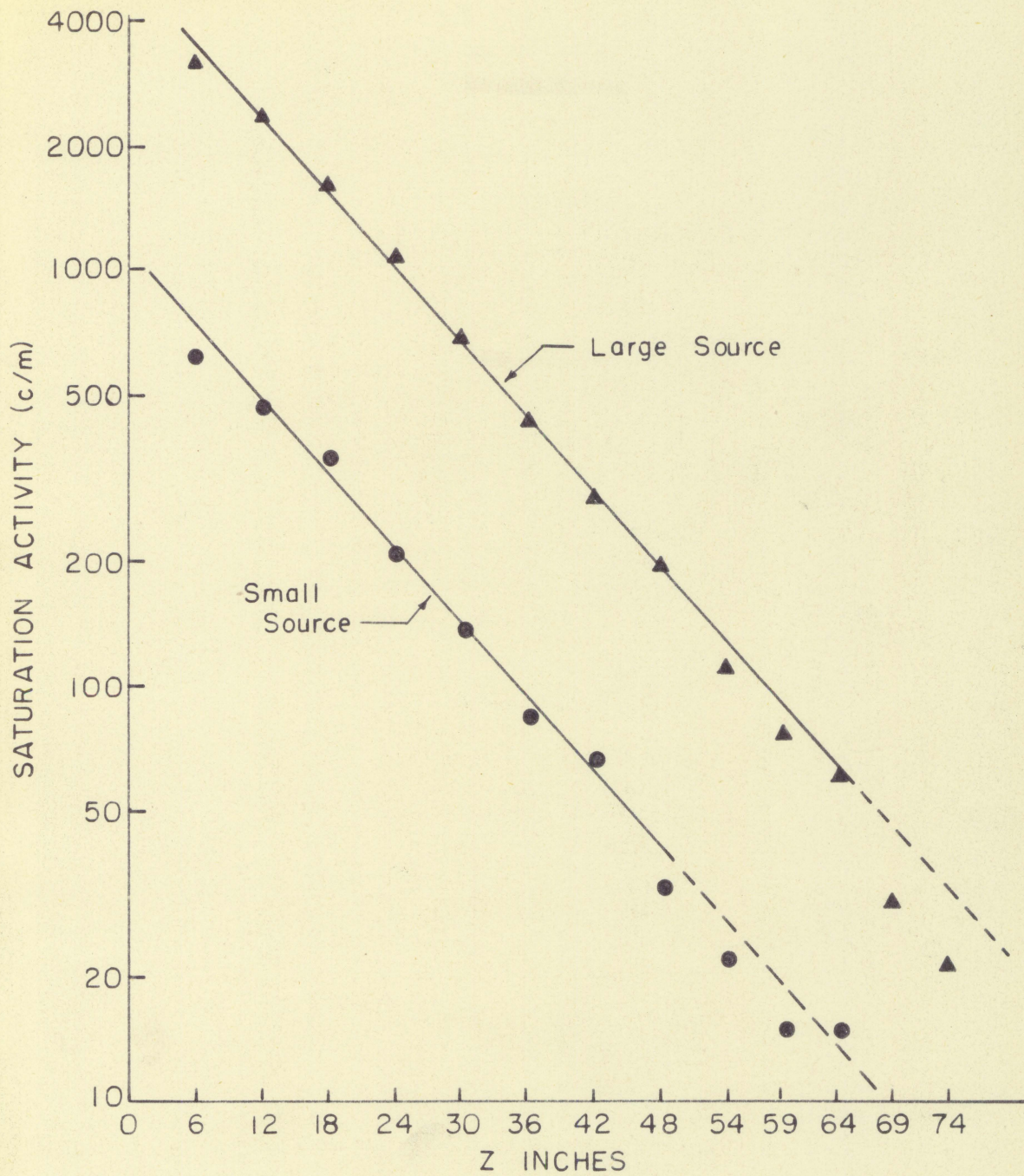


Figure 13. Vertical survey, 8.5 inch lattice, different neutron sources



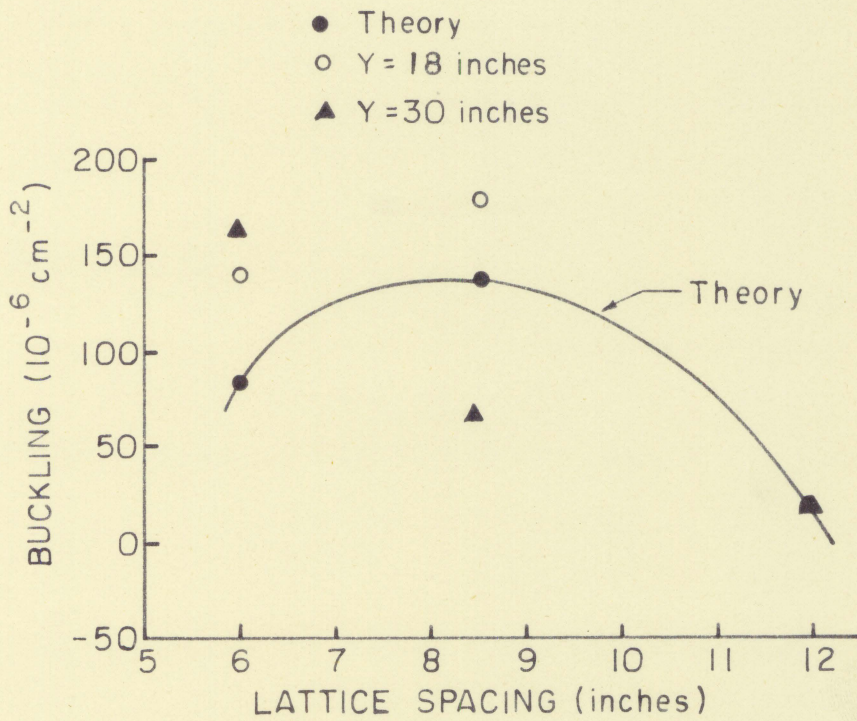


Figure 14. Buckling versus lattice spacing



Table 2. Experimental values of critical buckling  
"cm<sup>-2</sup>"

Configuration	6 in. lattice	8.5 in. lattice	12 in. lattice
Small neutron source, x = 27 in., y = 18 in.	$141 \times 10^{-6}$	$181 \times 10^{-6}$	Not determined
Small neutron source, x = 27 in., y = 30 in.	$161 \times 10^{-6}$	$65 \times 10^{-6}$	$19 \times 10^{-6}$
Large neutron source, x = 27 in., y = 30 in.	Not determined	$65 \times 10^{-6}$	Not determined

made to estimate buckling for the 12 in. lattice as the experimental points are too badly scattered. This is believed due to the equipment failure mentioned previously.

Figure 12 presents the same comparisons at  $y = 30$  in. This time the data for the 12 in. lattice appeared to be more reliable, and buckling was computed for all three lattices. Figure 13 presents the data for the 8.5 in. lattice from Figure 12, and compares it with data obtained for the same lattice with the large external neutron source. Parallel straight lines have been plotted for the two sets of data, and the experimental points fit these lines very well. It is noted that the slope of these lines gives a lower value of buckling for the 8.5 in. lattice at  $y = 30$  in. than did the data of Figure 11 taken at  $y = 18$  in.

It should be noted that a very small change in the slope of a line makes a marked difference in the value of critical



buckling computed from that slope. For this reason, repeated experiments at a high flux level would be necessary before completely reliable values of critical buckling could be determined for a given lattice arrangement. The experimental critical bucklings shown in Figure 14 should be considered to be indicative of general magnitude rather than highly accurate values.



## CONCLUSIONS

The operating characteristics of the subcritical assembly under investigation agree quite well with the accepted theory. The 8.5 in. lattice is the optimum lattice, resulting in higher flux levels and the largest value of critical buckling. All experimental buckling determinations proved to be positive, which indicates that a full scale reactor could be constructed of the same configuration as either the 6 in., 8.5 in., or 12 in. lattice. There is no apparent measurable flux depression due to indium foil loading, even when foils are loaded unsymmetrically. Horizontal flux distributions are symmetrical in both the x and the y directions, and within the limitations imposed by statistics they agree well with the cosine distributions predicted by theory.

The subcritical assembly could be operated satisfactorily using the smaller (100 millicurie) external neutron source. However, the scattering of the experimental points obtained with this source is quite severe, and statistical deviations are very large. With the larger neutron source in place, flux levels are higher by a factor of five or more, with correspondingly smaller deviations and less scattering of experimental points.

The fast neutrons from the external source are not entirely thermalized until they have penetrated approximately 30 in. into the assembly.



This subcritical assembly, with the large external neutron source in place, can be used to great advantage as an instructional tool. Although the experimental results obtained were not extremely accurate, it is believed that the data can be reproduced with sufficient consistency and accuracy to correlate experimental results with classroom calculations.



## SUGGESTIONS FOR FURTHER STUDY

Further study utilizing the same subcritical assembly used in this work might well be carried out in one of three general directions.

In the first of these categories lies the determination of various other properties of the assembly, such as diffusion length, Fermi age, and effective cross section. Methods of determining these quantities experimentally are given by Murray (7, p. 105). None of these properties has been determined experimentally for this particular subcritical assembly.

The second group of possible experiments includes all those in which some basic physical parameter is varied and the effect on nuclear properties is observed. Experiments such as the study of local flux depressions under various partial fuel loads, simulation of coolants, temperature effects on nuclear properties, variation of neutron source geometry, and simulation of control rods all come under this classification. For any lattice spacing other than 6 in. there is an appreciable volume of air contained in the empty fuel channels. Flux measurements should be made with these fuel channels filled with graphite to determine the effect, if any, of the empty channels.

The last type of experiment for which the subcritical assembly might be used is one in which the assembly acts as a testing facility, rather than being investigated itself.



This might include feasibility studies of a new type of neutron counter, or the development of a movable, continuously monitoring and recording survey instrument. This also could include the experimental justification of newly developed theory. An example of this type of application is the development of some new and less critical method of experimentally determining critical buckling.



## LITERATURE CITED

1. Smyth, Henry DeWolf. A general account of the development of methods of using atomic energy for military purposes under the auspices of the United States government 1940-1945. Wash., D.C., U. S. Government Printing Office. 1945.
2. United Nations. Proceedings of the International Conference on the Peaceful Uses of Atomic Energy. vol. 5. N. Y., United Nations. 1956.
3. Campbell, Edward C., L. D. Wyly, and E. I. Howell. Measurements on the orsort uranium graphite exponential pile. Atomic Energy Commission Document 3169. Oak Ridge, Tenn., U. S. Atomic Energy Commission. 1951.
4. Glasstone, Samuel and Milton C. Edlund. The elements of nuclear reactor theory. Princeton, N. J., D. Van Nostrand Co. 1956.
5. Kaplan, Irving. Nuclear physics. Cambridge, Mass., Addison-Wesley. 1956.
6. Glasstone, Samuel. Principles of nuclear reactor engineering. Princeton, N. J., D. Van Nostrand Co. 1956.
7. Murray, Raymond L. Nuclear reactor physics. Englewood Cliffs, N. J., Prentice-Hall. 1957.



## ACKNOWLEDGMENTS

The author wishes to thank Dr. Glenn Murphy for the original suggestion of this project and for his continued interest and assistance. To Dr. Adolf Voigt are due many thanks for allowing the use of the 100 millicurie radium-beryllium source, without which the experimental work could not have been completed without serious delay. Sincere gratitude is expressed to Dr. Robert E. Uhrig for his suggestions and encouragement throughout the entire course of the work.

This work at Iowa State College was the final year of a three year Aeronautical Engineering curriculum at the United States Naval Postgraduate School, Monterey, California. The author, therefore, would like to express his sincere appreciation to the U. S. Naval Postgraduate School and to the United States Navy for making this work possible.



APPENDIX



Table 3. Key to tables in Appendix

Table	Run	Neutron source	Lattice spacing	Comments
4	1	small	6 in.	
5	2	small	6 in.	Cadmium covered
6	3	small	6 in.	Light foil load
7	4	small	8.5 in.	
8	5	small	12 in.	
9	6	large	none	All fuel removed
10	7	large	8.5 in.	



Table 4. Run 1

Position	Saturated activity(c/m)	Position	Saturated activity(c/m)
A-5-0	4	F-5-30	115
A-5-6	5	G-5-0	14
A-5-12	15	G-5-6	37
A-5-18	21	G-5-12	64
A-5-24	25	G-5-18	73
A-5-30	26	G-5-24	91
B-5-0	0	G-5-30	102
B-5-6	11	H-5-0	2
B-5-12	21	H-5-6	29
B-5-18	38	H-5-12	43
B-5-24	49	H-5-18	57
B-5-30	43	H-5-24	62
C-5-0	10	H-5-30	80
C-5-6	23	I-5-0	4
C-5-12	46	I-5-6	19
C-5-18	66	I-5-12	41
C-5-24	75	I-5-18	42
C-5-30	89	I-5-24	47
D-5-0	6	I-5-30	54
D-5-6	25	J-5-0	1
D-5-12	50	J-5-6	6
D-5-18	73	J-5-12	14
D-5-24	99	J-5-18	16
D-5-30	99	J-5-24	25
E-5-0	7	J-5-30	29
E-5-6	38	E-13-0	0
E-5-12	72	E-13-6	3
E-5-18	76	E-13-12	0
E-5-24	105	E-13-18	1
E-5-30	129	E-13-24	4
F-5-0	10	E-13-30	4
F-5-6	24	E-12-0	4
F-5-12	68	E-12-6	6
F-5-18	80	E-12-12	6
F-5-24	91	E-12-18	5



Table 4. (Continued)

Position	Saturated activity(c/m)	Position	Saturated activity(c/m)
E-12-24	6	E-6-18	50
E-12-30	8	E-6-24	74
E-11-0	0	E-6-30	85
E-11-6	0	E-4-0	14
E-11-12	2	E-4-6	52
E-11-18	10	E-4-12	87
E-11-24	8	E-4-18	106
E-11-30	8	E-4-24	170
E-10-0	1	E-4-30	188
E-10-6	7	E-3-0	11
E-10-12	16	E-3-6	70
E-10-18	17	E-3-12	117
E-10-24	19	E-3-18	195
E-10-30	19	E-3-24	256
E-9-0	0	E-3-30	269
E-9-6	9	E-2-0	18
E-9-12	21	E-2-6	71
E-9-18	15	E-2-12	141
E-9-24	20	E-2-18	236
E-9-30	25	E-2-24	341
E-8-0	7	E-2-30	368
E-8-6	10	E-1-0	18
E-8-12	22	E-1-6	96
E-8-18	22	E-1-12	187
E-8-24	29	E-1-18	315
E-8-30	38	E-1-24	446
E-7-0	3	E-1-30	504
E-7-6	10		
E-7-12	24		
E-7-18	25		
E-7-24	42		
E-7-30	52		
E-6-0	4		
E-6-6	20		
E-6-12	63		



## 5. Run 2

osition	Saturated activity(c/m)	Position	Saturated activity(c/m)
E-8-30	16	E-3-30	89
E-9-30	12	E-2-30	156
E-10-30	1	E-1-30	201
E-11-30	7		
E-12-30	0		
E-13-30	4		
E-7-30	17		
E-6-30	24		
E-5-30	31		
E-4-30	51		

Table 6. Run 3

Position	Saturated activity(c/m)	Position	Saturated activity(c/m)
E-13-30	4	G-5-30	106
E-12-30	7	F-5-30	103
E-11-30	14	E-5-30	122
E-10-30	15	E-4-30	176
E-9-30	24	E-3-30	268
E-8-30	34	E-2-30	389
E-7-30	47	E-1-30	525
A-5-30	19		
B-5-30	47		
C-5-30	82		
J-5-30	16		
I-5-30	46		
H-5-30	70		
E-6-30	75		
D-5-30	99		



Table 7. Run 4

Position	Saturated activity(c/m)	Position	Saturated activity(c/m)
E-13-18	1	G-5-18	93
E-13-30	3	G-5-30	103
E-12-18	9	F-5-18	108
E-12-30	2	F-5-30	132
E-11-18	6	E-5-18	100
E-11-30	15	E-5-30	139
E-10-18	12	E-4-18	152
E-10-30	15	E-4-30	204
E-9-18	21	E-3-18	218
E-9-30	22	E-3-30	352
E-8-18	39	E-2-18	310
E-8-30	33	E-2-30	475
E-7-18	46	E-1-18	398
E-7-30	66	E-1-30	610
E-6-18	67	E-5-0	12
E-6-30	83	E-5-6	47
A-5-18	34	E-5-12	74
A-5-30	19	E-5-24	126
B-5-18	46	E-5-36	129
B-5-30	69	E-5-42	120
C-5-18	71	E-5-48	80
C-5-30	115	E-5-54	45
D-5-18	85	E-5-60	20
D-5-30	129		
J-5-18	23		
J-5-30	18		
I-5-18	56		
I-5-30	58		
H-5-18	72		
H-5-30	97		



Table 8. Run 5

Position	Saturated activity(c/m)	Position	Saturated activity(c/m)
E-13-18	8	J-5-30	18
E-13-30	6	I-5-18	52
E-12-18	6	I-5-30	59
E-12-30	8	H-5-18	70
E-11-18	14	H-5-30	102
E-11-30	7	G-5-18	103
E-10-18	12	G-5-30	126
E-10-30	17	F-5-18	104
E-9-18	18	F-5-30	143
E-9-30	22	E-5-18	100
E-8-18	28	E-5-30	135
E-8-30	46	E-4-18	203
E-7-18	38	E-4-30	241
E-7-30	49	E-3-18	260
E-6-18	62	E-3-30	374
E-6-30	89	E-2-18	348
A-5-18	18	E-2-30	559
A-5-30	19	E-1-18	405
B-5-18	48	E-1-30	663
B-5-30	58		
C-5-18	70		
C-5-30	90		
D-5-18	92		
D-5-30	113		
J-5-18	14		



Table 9. Run 6

Position	Saturated activity(c/m)	Position	Saturated activity(c/m)
E-13-30	9	J-5-30	135
E-12-30	22	E-5-0	70
E-11-30	33	E-5-6	235
E-10-30	53	E-5-12	399
E-9-30	73	E-5-18	555
E-8-30	149	E-5-24	660
E-7-30	243	E-5-30	684
E-6-30	399	E-5-36	654
E-4-30	1167	E-5-42	537
E-3-30	1842	E-5-48	392
E-2-30	2645	E-5-54	240
E-1-30	3535	E-5-60	76.5
A-5-30	129		
B-5-30	316		
C-5-30	469		
D-5-30	618		
F-5-30	699		
G-5-30	617		
H-5-30	477		
I-5-30	302		



Table 10. Run 7

Position	Saturated activity(c/m)	Position	Saturated activity(c/m)
E-13-30	22	J-5-30	141
E-12-30	30	E-5-0	86
E-11-30	61	E-5-6	244
E-10-30	78	E-5-12	398
E-9-30	110	E-5-18	531
E-8-30	193	E-5-24	650
E-7-30	288	E-5-30	702
E-6-30	438	E-5-36	689
E-4-30	1094	E-5-42	541
E-3-30	1600	E-5-48	394
E-2-30	2330	E-5-54	224
E-1-30	3115	E-5-60	59
A-5-30	138		
B-5-30	316		
C-5-30	492		
D-5-30	582		
F-5-30	723		
G-5-30	644		
H-5-30	486		
I-5-30	319		